Nucleon Gravitational Form Factors: Theory, Computation, and Experimental Extraction

Kiminad A. Mamo
University of Connecticut

The Center for Nuclear Femtography (CNF) and Theory Center mini-workshop
Vector Quarkonia as Pressure Gauges

March 27, 2026 Jefferson Lab

Roadmap

Across the two days, the workshop has already covered

- **Experiment:** threshold charmonium, CLAS12 J/ψ and ϕ, dileptons, and what can actually be measured.
- **Analysis:** amplitude analyses, neural-network CFF fits, Gaussian-process tools, and uncertainty quantification.
- **Theory/computation:** GFFs from lattice, transition GPDs, and factorization frameworks.

So the right closing viewpoint is

$$\text{GPDs} \longrightarrow \text{moments} \longrightarrow \text{GFFs} \longrightarrow \text{quarkonium extraction}$$

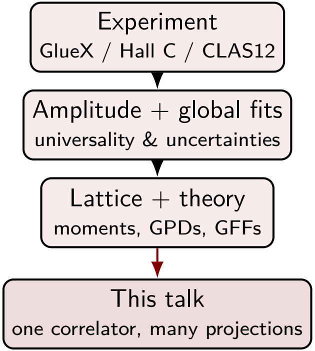

Roadmap

1. **Theory and computation**
   - GPDs at $\eta = 0$: impact-parameter parton densities.
   - GPDs at $\eta \neq 0$: off-forward parton–nucleon correlations.
   - Spin-2 moments $\Rightarrow$ GFFs A, B, D.
   - Soft-wall holographic computation and comparison to lattice.
2. **Experimental extraction**
   - Why near-threshold J/ψ is a gluonic filter.
   - How the amplitude isolates $A_g(t)$ and $D_g(t)$.
   - What "vector quarkonia as pressure gauges" should really mean.

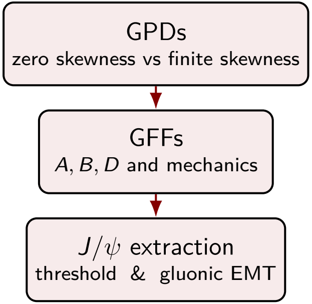

Take-home message up front

Density language at $\eta = 0$; correlation language at $\eta \neq 0$.

GPDs: one object, many projections

Leading-twist quark/gluon GPDs

$$F(x,\eta,t) \sim \int \frac{\mathrm{d}z^-}{2\pi}\, \mathrm{e}^{\mathrm{i}xP^+z^-} \langle p'|\bar{\psi}(-z/2)\,\Gamma\, W\, \psi(z/2)|p\rangle.$$

- x: longitudinal momentum fraction.
- η: skewness / off-forwardness / rapidity gap.
- t: invariant momentum transfer.

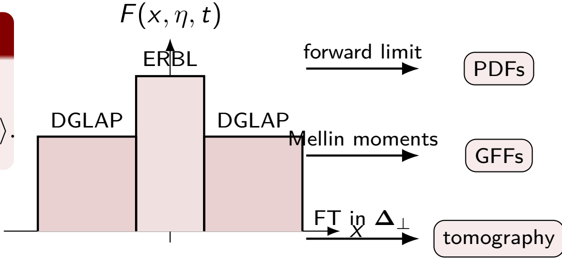

The real question is: what does tomography mean once $\eta \neq 0$?

Three familiar limits

$F(x,0,0) \to$ PDFs, $\int \mathrm{d}x\, x^{n-1} F \to$ form factors, $\int \frac{\mathrm{d}^2\boldsymbol{\Delta}_\perp}{(2\pi)^2}\, \mathrm{e}^{-\mathrm{i}\boldsymbol{\Delta}_\perp\cdot\boldsymbol{b}_\perp} F \to$ spatial tomography.

At zero skewness: impact-parameter densities in the IMF

Burkardt picture at $\eta = 0$

$$q(x, \boldsymbol{b}_\perp) = \int \frac{\mathrm{d}^2\boldsymbol{\Delta}_\perp}{(2\pi)^2}\, \mathrm{e}^{-\mathrm{i}\boldsymbol{\Delta}_\perp \cdot \boldsymbol{b}_\perp} H(x, 0, -\boldsymbol{\Delta}_\perp^2)$$

for a proton localized in the transverse plane and viewed in the infinite-momentum frame.

- The transform admits positivity constraints, so for $x > 0$ it can be interpreted as a parton probability density in transverse space.
- The density language is tied to **state preparation**: transverse localization, diagonal longitudinal momentum, and the IMF viewpoint.
- Second moments image longitudinal momentum flow; E controls transverse distortions for polarized targets.

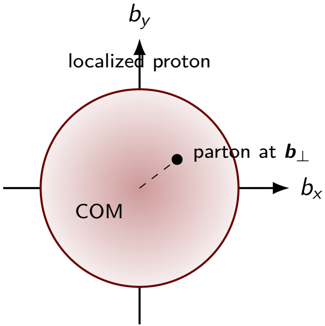

Density statement

At $\eta = 0$, the Fourier transform is diagonal in the hadron state and admits a genuine partonic density interpretation.

At finite skewness: off-forward correlation, not probability

What changes when $\eta \neq 0$?

$$\rho(x, \boldsymbol{b}_\perp; \eta) = \int \frac{\mathrm{d}^2\boldsymbol{\Delta}_\perp}{(2\pi)^2}\, \mathrm{e}^{-\mathrm{i}\boldsymbol{\Delta}_\perp\cdot\boldsymbol{b}_\perp} F\left(x, \eta, -\frac{\boldsymbol{\Delta}_\perp^2 + 4\eta^2 M_N^2}{1-\eta^2}\right)$$

connects *different* hadron momentum eigenstates.

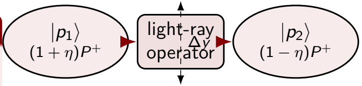

- The initial and final proton carry $p_1^+ = (1+\eta)P^+$ and $p_2^+ = (1-\eta)P^+$.
- The rapidity gap is

$$\Delta y = \ln\frac{1+\eta}{1-\eta} = 2\,\mathrm{artanh}(\eta).$$

- The norm is fixed at $t = -c_\eta$, with $N_n(\eta) = H_n(\eta, -c_\eta)$.

Diehl 2002; Hechenberger–Mamo–Zahed 2026

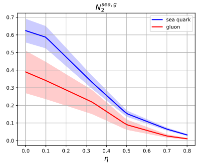

Actual depletion of $N_2^{\mathrm{sea},g}(\eta)$ with rapidity gap.

Interpretation

At finite skewness, the Fourier transform is a parton–nucleon correlation amplitude in transverse space.

Spin-2 moments, GFFs, and why $\eta = 0$ matters

Second moments define the gravitational form factors

$$H_a^{(+)}(2, \eta, t) = A_a(t) + \eta^2 D_a(t), \qquad E_a^{(+)}(2, \eta, t) = B_a(t) - \eta^2 D_a(t).$$

	$\eta = 0$	$\eta \neq 0$
State	IMF, localized	off-forward / rapidity gap
FT	density	correlation
Spin	$J_a = \frac{1}{2}[A_a(0) + B_a(0)]$	$J_a(\eta) = \frac{1}{2}[A_a(-c_\eta) + B_a(-c_\eta)]$
Mechanics	density language	stress correlation

Finite-gap Ji logic: D cancels in $H + E$ at fixed t; the observed η-dependence comes from evaluating the off-forward correlation at $t = -c_\eta = \frac{4\eta^2 m_N^2}{1-\eta^2}$.

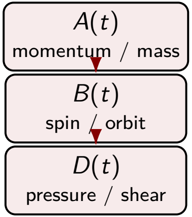

Outside the $\eta = 0$ IMF limit, the mechanical image is not a literal parton density.

Soft-wall setup

$$ds^2 = \frac{R^2}{z^2}(\eta_{\mu\nu}\,dx^\mu dx^\nu - dz^2), \qquad \phi(z) = \kappa^2 z^2.$$

- Tensor 2^{++} exchange gives the spin-2 channel and fixes $A(t)$.
- Scalar 0^{++} exchange completes the trace channel and therefore fixes the combination that determines $D(t)$.
- The bulk computation is naturally *off-forward*: source, sink, and exchanged bulk field define a genuine correlation before any $\eta \to 0$ density limit is taken.

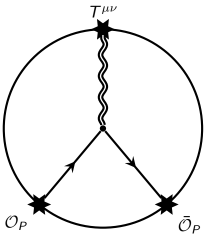

$2^{++} \Rightarrow A(t)$

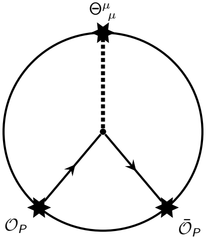

$0^{++} \Rightarrow D(t)$

Soft-wall outputs: $A_g(t)$ and $D_g(t)$ versus lattice

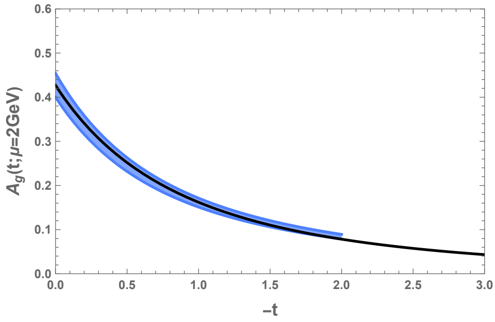

Spin-2 / tensor channel: $A_g(t)$

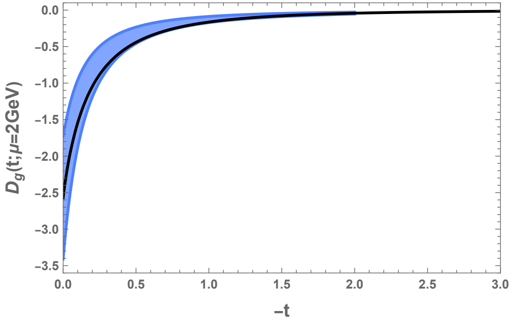

Scalar completion / D-term channel: $D_g(t)$

Computational logic

Forward limits come from PDFs; Regge slopes from spectroscopy and form-factor systematics; polynomiality is imposed in moment space; after NLO evolution, the $j = 2$ moments show qualitative — and in several channels fair — agreement with current lattice data.

- Heavy quarkonium behaves as a compact color dipole and filters **gluonic** dynamics.
- Near threshold, the amplitude is especially sensitive to the lowest moments of gluon GPDs — precisely the gluonic EMT form factors.
- At higher energy the same object reggeizes; threshold and diffraction are different kinematic windows on closely related correlators.

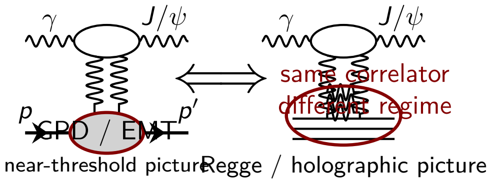

Process

$$\gamma p \to J/\psi\, p, \qquad W^2 = s, \qquad t = (p' - p)^2.$$

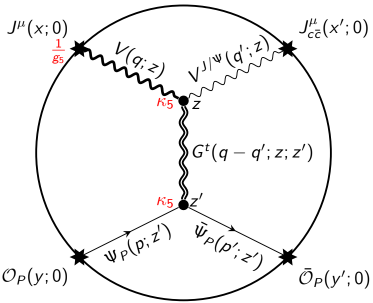

From the amplitude to the extraction of $A_g(t)$ and $D_g(t)$

Near-threshold structure of the cross section

$$\frac{\mathrm{d}\sigma}{\mathrm{d}t} \propto \frac{1}{32\pi(s - M_N^2)^2} F(s, t, M_{J/\psi}, M_N)\left[A_g(t)+\eta^2 D_g(t)\right]^2.$$

- 2^{++} exchange determines the tensor channel $A_g(t)$.
- The scalar completion is essential: without the D-term, the near-threshold extraction is incomplete.
- This is the experimental face of the same moment decomposition used on the theory side.

$$A_g^S(t) = A_g(t) - \frac{3t}{4M_N^2} D_g(t)$$

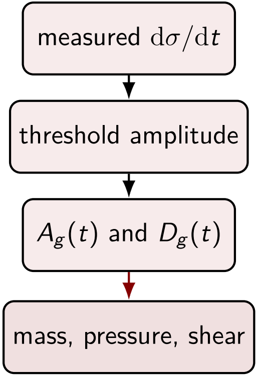

Tensor channel + scalar completion ⇒ mechanical interpretation.

Recent CLAS12 extraction: gluonic $A_g(t)$ and $C_g(t)$

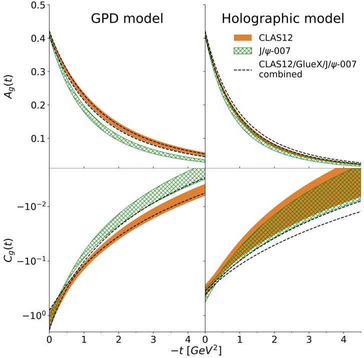

The recent CLAS12 extraction shows both $A_g(t)$ and $D_g(t) = 4C_g(t)$ in GPD and holographic fits.

From $D_g(t)$ to pressure and shear — but keep the interpretation honest

Mechanical distributions

$$p(r),\ s(r)\ \propto \int \frac{d^3\boldsymbol{\Delta}}{(2\pi)^3}\, e^{i\boldsymbol{\Delta}\cdot\boldsymbol{r}}\, D(t), \qquad t = -\boldsymbol{\Delta}^2$$

- $D(t)$ controls the stress tensor and therefore the pressure and shear patterns.
- In the usual Breit-frame mechanical language, these are best understood as spatial images of an **off-forward stress correlation**.
- So the *"pressure "* interpretation is sensible precisely because quarkonium measures this correlator — not because it directly photographs a static fluid.

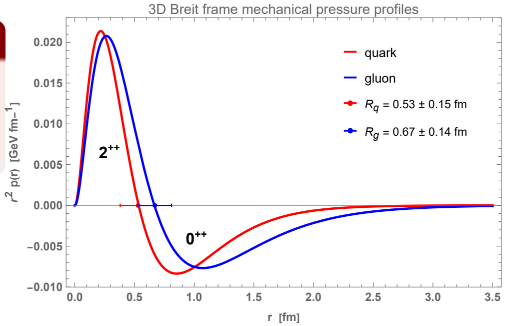

Key caution

Density language is sharpest at $\eta = 0$ in the IMF; mechanical language away from that limit should be read as a correlation-space statement.

Total cross section of J/ψ photoproduction from near threshold to high energy

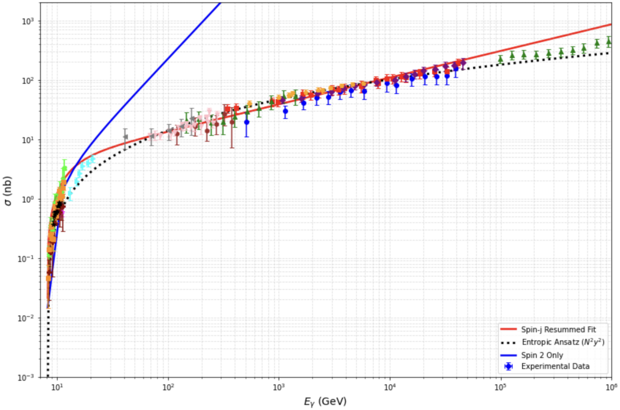

Figure: Total J/ψ photoproduction cross section in holographic QCD, fit from threshold to high energy.

Vision after this workshop: close the loop, do not split the program

- **Theory/computation:** all-skewness GPD engines must preserve support, polynomiality, and analyticity.
- **Lattice:** moments and GFFs remain the cleanest nonperturbative anchor for A, B, D.
- **Experiment:** threshold photo/electroproduction and eventually ϕ and Υ channels should test the universality of the extracted gluonic correlators.
- **Global analysis:** the real target is one framework linking DVCS, vector mesons, lattice moments, and GFF extractions.

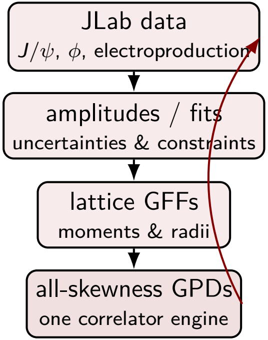

Vision

Treat threshold quarkonium, lattice moments, and all-skewness GPD phenomenology as one program.

Summary

- At $\eta = 0$, the transverse Fourier transform of a GPD has a clean impact-parameter density interpretation in the IMF.
- At $\eta \neq 0$, the same object is an off-forward parton–nucleon correlation; its norm is fixed at $t = -c_\eta$ and decreases with rapidity gap.
- Spin-2 moments define the GFFs A, B, D; pressure and shear are controlled by $D(t)$, but their spatial images are best read as correlation-space observables away from the $\eta = 0$ density limit.
- Soft-wall holographic QCD gives a concrete computational picture: 2^{++} and 0^{++} Witten diagrams compute the tensor and scalar channels and compare nontrivially with lattice.
- Near-threshold J/ψ is therefore not just a qualitative "pressure picture" tool — it is a realistic experimental handle on the gluonic stress correlator of the nucleon.

Closing line

Vector quarkonia are best viewed as precision probes of off-forward gluonic stress correlations.

Thank you

Backup: tomography from the recent finite-skewness paper

model the conformal moments by a "Reggeized" Mellin transform,

$$\mathcal{F}_a(j,t;\mu_0) \equiv \mathbb{F}_a(j,0,t;\mu_0) = \int_0^1 \mathrm{d}x\, \frac{f_a(x,\mu_0)}{x^{\,j-1+\alpha'_a t}}, \qquad (5)$$

where f_a are the empirical forward PDFs at μ_0 and α'_a are linear Regge slopes. We use the MSTW09 NLO set for unpolarized PDFs [23] and the AAC NLO set for polarized PDFs [24], which allow analytic Mellin transforms in Eq. (5) and match the Regge calibrations used in Refs. [13, 14].

The slopes used in this work are collected in Table I. For some channels a secondary trajectory with slope α'^{S}_a is introduced to cancel spurious poles in the finite-skewness continuation (see Sec. III C).

C. Finite skewness and analytic continuation

To extend the moments to $\eta \neq 0$ we use the unique hypergeometric kernel derived in cubic string field theory that enforces polynomiality, crossing symmetry, and removes spurious poles [13, 25].[1] We then obtain:

$$\mathbb{F}_a(j,\eta,t;\mu_0) = \left[\hat{d}_j(\eta,t) - 1\right]\left[\mathcal{F}_a(j,t;\mu_0) - \mathcal{F}^{\mathrm{S}}_a(j,t;\mu_0)\right] + \mathcal{F}_a(j,t;\mu_0), \qquad (6)$$

with

$$\hat{d}_j(\eta,t) = {}_2F_1\!\left(\tfrac{1}{2} - j,\, -\tfrac{j}{2}; \tfrac{1}{2}; -\tfrac{4m_N^2\eta^2}{t}\right). \qquad (7)$$

Here ${}_2F_1$ is the Gauss hypergeometric function and $\mathcal{F}^{\mathrm{S}}_a(j,t)$ denotes the secondary trajectory contribution obtained from Eq. (5) by $\alpha'_a \to \alpha'^{\mathrm{S}}_a$. This construction guarantees the correct ERBL/DGLAP support and polynomiality of Mellin moments at any skewness, while retaining an analytic structure controlled by linear trajectories.

D. Evolution and MB inversion

All leading-twist singlet and non-singlet moments $\{\mathbb{H}, \mathbb{E}, \widetilde{\mathbb{H}}\}$ are evolved from μ_0 to a generic scale μ by solving the NLO DGLAP–ERBL evolution equations directly in conformal space. The x-space GPDs at any (x,η,t) are then obtained by numerical MB inversion of Eq. (4).

As an illustration, Fig. 1 shows selected non-singlet/isovector channels reconstructed with a single Regge parameter set, compared to lattice results. The orange curve is consistent within uncertainties, while the green curves (both panels) and the blue curve (bottom) exhibit visible tension. Within our framework these deviations are driven primarily by the forward PDF priors and by residual systematics associated with the t-slopes entering Eq. (5); we return to this in Sec. V.

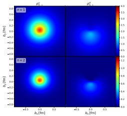

(a) $\eta = 0$

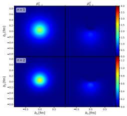

(b) $\eta = 0.33$

FIG. 2: Spatial tomography at $\mu = 2\,\mathrm{GeV}$ for non-singlet transverse densities $\rho_n^{u/d}(\boldsymbol{b}_\perp;\eta)$ (with $n = 1,2$) defined in Eq. (8) for a nucleon polarized along $+\hat{\boldsymbol{y}}$. Panel (a) shows $\eta = 0$ (impact-parameter densities). Panel (b) shows $\eta = 0.33$, corresponding to a rapidity gap $\Delta y = 2\,\mathrm{artanh}(\eta) \simeq 0.69$; the overall norms decrease according to Eq. (10).

[1] While finalizing this manuscript it was brought to our attention that aspects of the $\eta = 0$ construction overlap with other conformal parametrizations (e.g. Ref. [26]). In our framework the dynamical motivation and, crucially, the finite-skewness dependence through Eqs. (6)–(7) provide a clear discriminator.

Backup: rapidity dependence and modified Ji identities

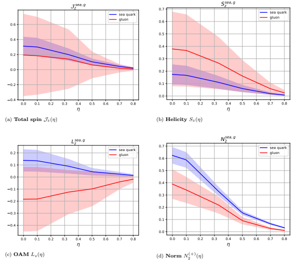

(a) **Total spin** $\mathcal{J}_z(\eta)$

(b) **Helicity** $S_z(\eta)$

(c) **OAM** $L_z(\eta)$

(d) **Norm** $N_2^{(+)}(\eta)$

FIG. 6: Rapidity dependence at $\mu = 2\,\mathrm{GeV}$ of (a) total spin $\mathcal{J}_z(\eta)$, (b) helicity $S_z(\eta)$, (c) orbital angular momentum $L_z(\eta)$, and (d) the correlation norm $N_2^{(+)}(\eta) = \mathbb{H}^{(+)}(2, \eta, -c_\eta)$ (cf. Eq. (10)). Spin observables are defined at $t = -c_\eta$ through Eq. (13). The horizontal axis is the rapidity gap Δy related to η by Eq. (1). Theory bands denote propagated PDF uncertainties.

kinematic point $t = -c_\eta$. We define the corresponding rapidity-dependent (effective) contributions

$$S_z^a(\eta; \mu) \equiv S_a^z(\eta, -c_\eta; \mu) = \tfrac{1}{2}\widetilde{\mathbb{H}}_a^{(+)}(1, \eta, -c_\eta; \mu), \quad (13a)$$

$$\mathcal{J}_z^a(\eta; \mu) \equiv \mathcal{J}_a^z(\eta, -c_\eta; \mu) = \tfrac{1}{2}\big[\mathbb{H}_a^{(+)}(2, \eta, -c_\eta; \mu) + \mathbb{E}_a^{(+)}(2, \eta, -c_\eta; \mu)\big], \quad (13b)$$

$$L_z^a(\eta; \mu) \equiv L_a^z(\eta, -c_\eta; \mu) = \mathcal{J}_z^a(\eta; \mu) - S_z^a(\eta; \mu). \quad (13c)$$

For the second moment, Lorentz covariance and polynomiality relate the conformal moments to the nucleon matrix elements of the (quark/gluon) energy–momentum tensor. In a standard parametrization one introduces gravitational form factors $A_a(t)$ and $B_a(t)$ and a D-term form factor $D_a(t)$ such that [7, 18]

$$\mathbb{H}_a^{(+)}(2, \eta, t; \mu) = A_a(t; \mu) + \eta^2 D_a(t; \mu), \quad (14a)$$

$$\mathbb{E}_a^{(+)}(2, \eta, t; \mu) = B_a(t; \mu) - \eta^2 D_a(t; \mu), \quad (14b)$$

so that the D-term cancels in the sum and

$$\mathbb{H}_a^{(+)}(2, \eta, t) + \mathbb{E}_a^{(+)}(2, \eta, t) = A_a(t) + B_a(t), \quad (15)$$

independent of η.

Evaluating the correlation at $\mathbf{\Delta}_\perp = 0$ therefore amounts to evaluating the form factors at $t = -c_\eta$, which decreases the total spin with increasing rapidity gap. Summing over quark and gluon channels gives the